International Journal of Fluid Machinery and Systems
Vol. 3, No. 1, January-March 2010

**Original Paper**

# A Two-Dimensional Study of Transonic Flow Characteristics in Steam Control Valve for Power Plant

**Koichi Yonezawa[1], Yoshinori Terachi[1], Toru Nakajima[1], Yoshinobu Tsujimoto[1]
Kenichi Tezuka[2], Michitsugu Mori[2], Ryo Morita[3] and Fumio Inada[3]**

[1]Graduate School of Engineering Science, Osaka University
1-3, Machikaneyama-cho, Toyonaka, Osaka, 560-8531, Japan
[2]Engineering R&D Division, Tokyo Electric Power Company
4-1, Egasaki-cho, Tsurumi-ku, Yokohama, Kanagawa, 230-8510, Japan
[3]Nuclear Energy Systems Department, Central Research Institute of Electric power Industry
2-11-1, Iwado Kita, Komae-shi, Tokyo, 201-8511, Japan

**Abstract**

A steam control valve is used to control the flow from the steam generator to the steam turbine in thermal and nuclear power plants. During startup and shutdown of the plant, the steam control valve is operated under a partial flow conditions. In such conditions, the valve opening is small and the pressure deference across the valve is large. As a result, the flow downstream of the valve is composed of separated unsteady transonic jets. Such flow patterns often cause undesirable large unsteady fluid force on the valve head and downstream pipe system. In the present study, various flow patterns are investigated in order to understand the characteristics of the unsteady flow around the valve. Experiments are carried out with simplified two-dimensional valve models. Two-dimensional unsteady flow simulations are conducted in order to understand the experimental results in detail. Scale effects on the flow characteristics are also examined. Results show three types of oscillating flow pattern and three types of static flow patterns.

**Keywords**: Transonic flow, Control valve, Flow oscillation

## 1. Introduction

In nuclear and thermal power plants, various flow control valves are used. The main steam control valve is one of the most important valves. The steam control valve is located between the steam generator and the high-pressure turbine. During startup and shutdown of the plant, the opening of the steam control valve is changed very slowly in order to reduce thermal stress in the system component. This includes the operation with small valve opening with large pressure difference. Under such conditions, flow around the valve becomes transonic and shock waves appear. As a result, the flow separates from the wall associated with a shock-boundary layer interaction. The separated transonic jet often becomes unstable and may cause undesirable fluctuations of the valve itself and pipe systems. Such fluctuations should be avoided in order to enhance reliability of power plants. About the flow fluctuation in the steam control valve in a steam turbine, several studies have been reported. Windel [1] reported the valve vibration in a large steam turbine caused by acoustic oscillation in the pipe downstream of the valve. Araki *et al*. [2] and Jibiki [3] reported investigations of unsteady behavior of separated transonic flow around the valve with subscale 2-D and 3-D experimental models. In the study of Araki *et al*. [2], it is reported that there are a self-excited oscillation and a forced oscillation of the valve head. Morita *et al*. [4] carried out experimental and numerical studies with sub-scale cold flow. In these reports, the detailed flow pattern around the valve head are observed with numerical results. However, there still remain several unclear points about the flow characteristics and its mechanisms.

In the present paper, experimental and numerical investigations with two-dimensional models are carried out as the first step of the study on the flow-induced vibration of the steam control valve. With the two-dimensional experimental model with rectangular cross-section, the flow pattern becomes simpler than that in a three-dimensional model with a circular cross section. By flow visualization with Schlieren method, flow patterns are identified under various conditions. The causes of the flow fluctuations are

Received December 9 2009; accepted for publication January 5 2010: Review conducted by Prof. Wang Lequin. (Paper number O09052)
Corresponding author: Koichi Yonezawa, Assistant Professor, yonezawa@me.es.osaka-u.ac.jp

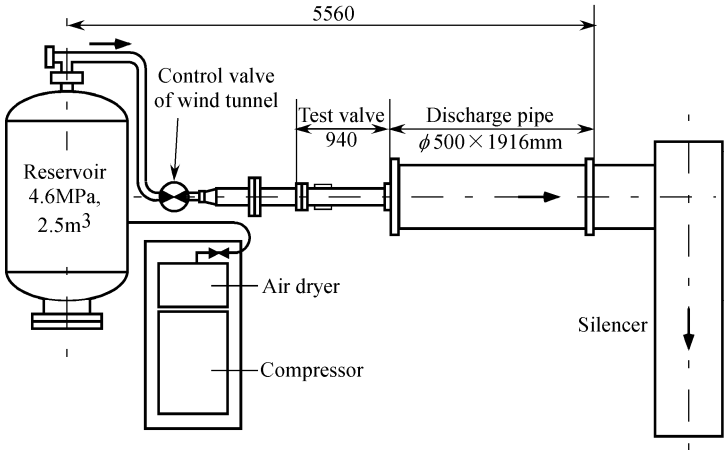


**Fig. 1** Schematic of blow-down wind tunnel

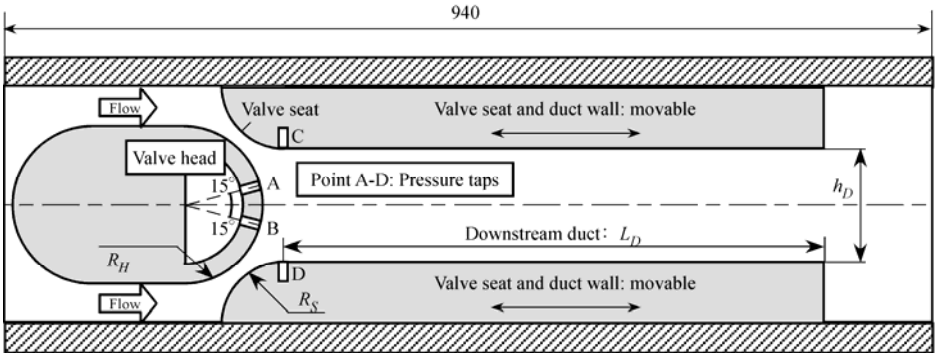


**Fig. 2** Schematic of test valve

**Table 1** Dimension of test valve

| | Smaller model [mm] | Larger model [mm] |
|---|---|---|
| Curvature radius of valve head: $R_H$ | 40 | 80 |
| Curvature radius of valve seat: $R_S$ | 32 | 64 |
| Height of downstream duct: $h_D$ | 64 | 128 |
| Length of downstream duct: $L_D$ | 400 | 600 |
| Depth of downstream duct: $w_D$ | 75 | 240 |

examined based on the numerical analysis. Scale effects are studied by experimental and numerical methods.

## 2. Experimental Apparatus

Air is used for the convenience of experiment, although the working fluid is steam in actual power plants. The overview of the wind tunnel is shown in Fig. 1. The dry and filtered air is stored in the high-pressure tank with the maximum pressure of 4.6MPa. The control valve adjusts the inlet pressure. The flow through the test valve is discharged to the atmosphere through the downstream pipe and the silencer with sufficiently large cross sections. The pressure loss downstream of the test valve is so small that we can consider the back pressure to be the atmospheric pressure.

The schematic of the two-dimensional test valve is shown in Fig. 2. Two similar valves with different scales are tested in order to examine scale effects. Major dimensions are shown in Table 1. The contours of the valve head and the valve seat consist of simple circular arcs. The larger model is twice as large as smaller model except for the duct length $L_D$ and the depth $w_D$. It is known that the flow becomes unstable when the flow separates from the valve seat [2][3]. Therefore, the valve head has larger curvature radius than that of the valve seat in order to simulate flow instabilities. The flow field around the valve is visualized with Schlieren setup (KATO KOUKEN, System Schlieren SS200) and a high speed video (Photron, FASTCAM-Ultima-SE). The flame rate is 13500 frames per second. Wall pressure was measured at four points A-D shown in Fig. 2 with semiconductor pressure transducers (KULITE, CCQ-093-200G for smaller model and CT-190-100A for larger model) and recorded with a digital data recorder (SONY, PC216Ax) with the sampling frequency of 12 kHz.

The operating condition of the valve is defined by two parameters. One is the valve opening ratio and the other is the pressure ratio. The valve opening ratio is defined as

$$\varepsilon_L = \frac{x_L}{D_S} \tag{1}$$

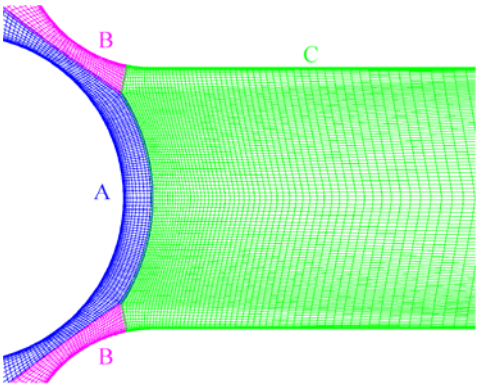


**Fig. 3** Computational grid for CFD

**Table 2** Number of grid node

| Block | Smaller model | Larger model |
|---|---|---|
| A | 177×30 | 377×45 |
| B | 30×31 | 100×46 |
| C | 251×137 | 251×267 |
| Total | 41577 | 93182 |

where $x_L$ is the valve lift defined as the axial displacement of the valve head from shut-off and $D_s$ is the seat diameter defined as the distance of upper and lower contact points of the valve head and the seat at shut-off. The seat diameter is given by following geometric relationship for the case of the present simple model.

$$D_S = \left( \frac{2R_S + h_D}{R_H + R_S} \right) R_H \tag{2}$$

Where $R_S$ is the curvature radius of the valve seat, $R_H$ is the radius of the valve head, and $h_D$ is the height of the duct.
The pressure ratio is obtained as follows.

$$\psi_p = \frac{p_2}{p_{01}} \tag{3}$$

Here, $p_{01}$ is the inlet total pressure and $p_2$ is outlet static pressure.

## 3. Numerical Method

Two-dimensional Navier-Stokes simulations are carried out in order to study the flow characteristics in detail. The numerical code is based on a finite difference method. A non-MUSCL type second order fully upwind TVD scheme by Harten and Yee[5] is applied for the numerical flux of convective terms. The viscous term is calculated with a second order central difference scheme. Modified sub-grid-scale (SGS) model of the large eddy simulation (LES) [6] are used as a turbulence model. Unsteady simulation is conducted with three-point backward difference scheme and LU-SGS methods [7]. This combination of the numerical schemes has been adopted for the numerical study of the unsteady flows in the steam control valve [4]. The numerical results show good agreement with experimental results. Additional validations of the accuracy in space and time are also shown in ref [4].

The computational grid for the larger model is shown in Fig. 3. The computational domain is shown in Fig. 2. The same topology is applied for the smaller model. The number of grid nodes in each block is shown in Table 2.

## 4. Results and Discussions

### 4.1 Classification of flow patterns

Flow patterns are classified based on the results of the flow visualizations and wall pressure measurements. The following results are obtained for larger and smaller models.

Attached flow

Fig. 4 shows the flow field and the pressure fluctuations for the case when both upper and lower jets attach on the duct wall almost symmetrically. The pressure fluctuation is not large without any specific frequency component as shown in Fig. 4 (b) and Fig. 4 (c).

Fig. 5 shows the flow field and the pressure fluctuations for the case when separated jets do not attach on walls symmetrically. The pressure ratio is smaller than the case of symmetrical attachment. As shown in Fig. 5 (a), upper jet attaches on the valve head and the lower jet reattaches on the downstream duct wall. As shown in Fig. 5 (b), the amplitude of the pressure fluctuation at point A is larger than that at point B because the upper jet attaches on the valve head. As shown in Fig. 5 (c), however, both fluctuations do not have a specific frequency. The asymmetry occurs rather randomly in each test but does not change during the test. In a three-dimensional model, however, the direction of such an asymmetric pattern rotates randomly in circumferential direction without specific frequencies [4].

Flow oscillation

Fig. 6 shows the flow field and the pressure fluctuations for the case when separated jets fluctuate periodically in lateral

direction. As shown in Fig. 6 (a), both separated jets fluctuate alternately. The wall pressure fluctuates with a large amplitude. The frequency of the wall pressure fluctuation is 1100Hz for the larger model. This frequency is almost the same as the 1st order mode of the acoustic resonance frequency in the height direction of the duct.

Such an asymmetric mode of flow oscillation appears accompanied by an axial mode oscillation at some conditions shown in Fig. 7. The axial mode is caused by an acoustic resonance in downstream duct [1].

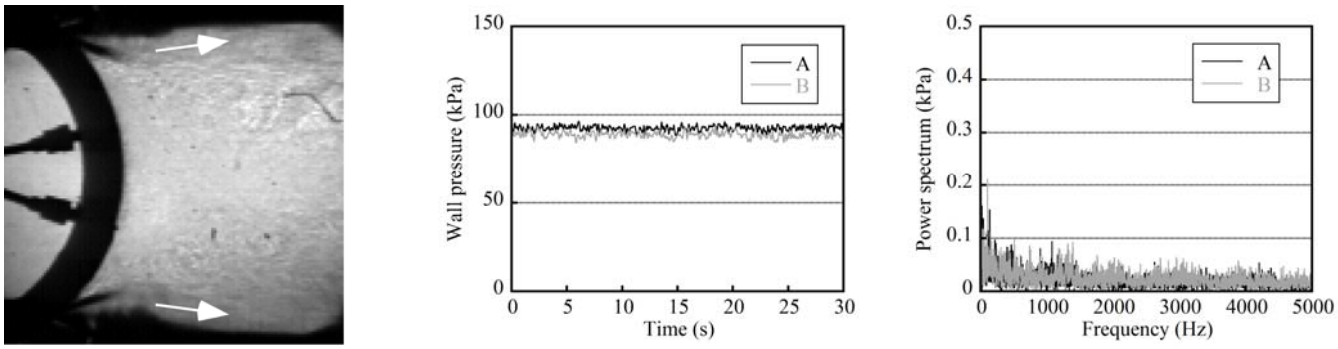


(a) Schlieren snap shot (b) Wall Pressure measurement of valve head (c) FFT result of pressure fluctuation of valve head

**Fig. 4** Flow visualization and wall pressure measurement (Larger model, $\varepsilon_L$=0.20, $\psi_p$=0.91)

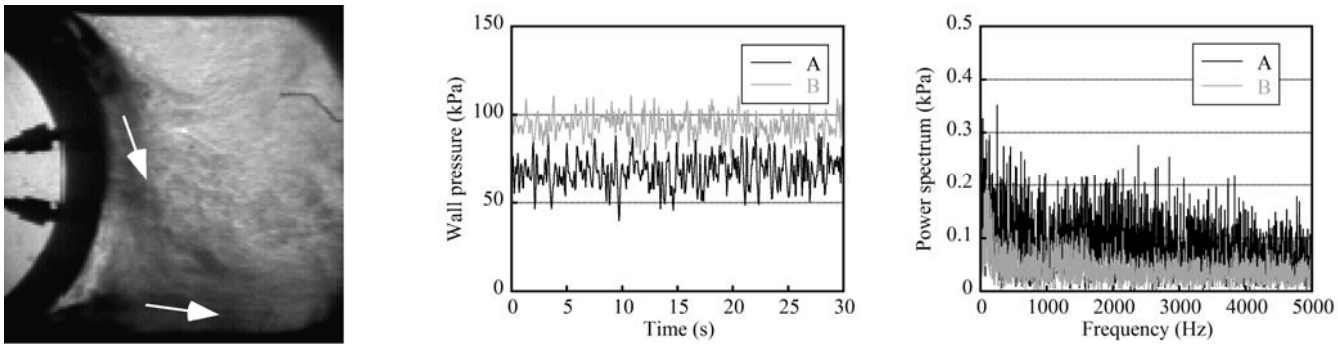


(a) Schlieren snap shot (b) Wall Pressure measurement of valve head (c) FFT result of pressure fluctuation of valve head

**Fig. 5** Flow visualization and wall pressure measurement (Larger model, $\varepsilon_L$=0.10, $\psi_p$=0.40)

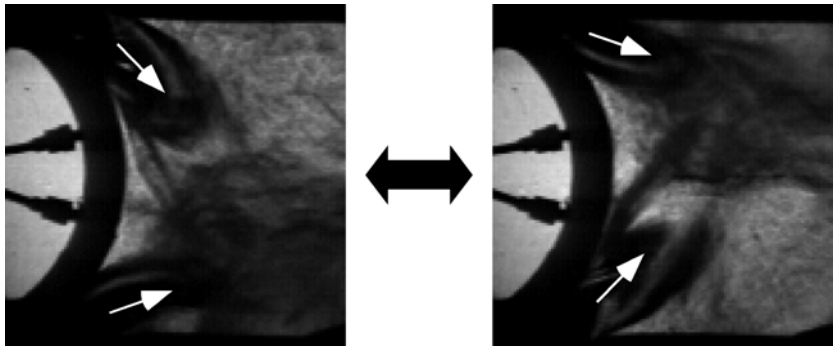

(a) Schlieren snap shots of one-cycle of flow fluctuation

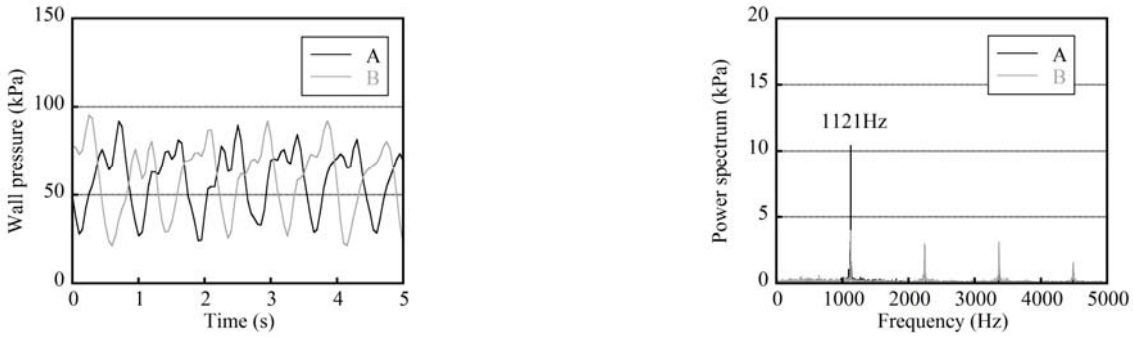


(b) Wall Pressure measurement of valve head (c) FFT result of pressure fluctuation of valve head

**Fig. 6** Flow visualization and wall pressure measurement (Larger model, $\varepsilon_L$=0.20, $\psi_p$=0.36)

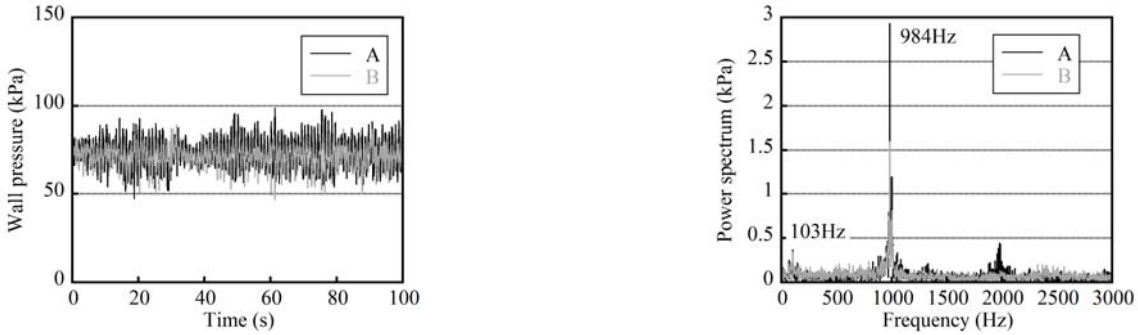


(a) Wall Pressure measurement of valve head (b) FFT result of pressure fluctuation of valve head

**Fig. 7** Wall pressure measurement (Larger model, $\varepsilon_L$=0.15, $\psi_p$=0.43)

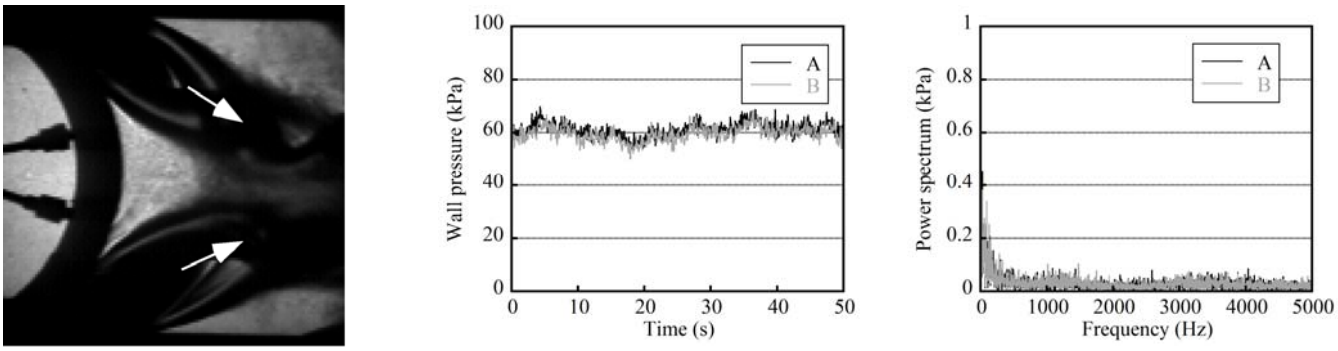


(a) Schlieren snap shot (b) Wall Pressure measurement of valve head (c) FFT result of pressure fluctuation of valve head

**Fig. 8** Flow visualization and wall pressure measurement (Larger model, $\varepsilon_L$=0.20, $\psi_p$=0.29)

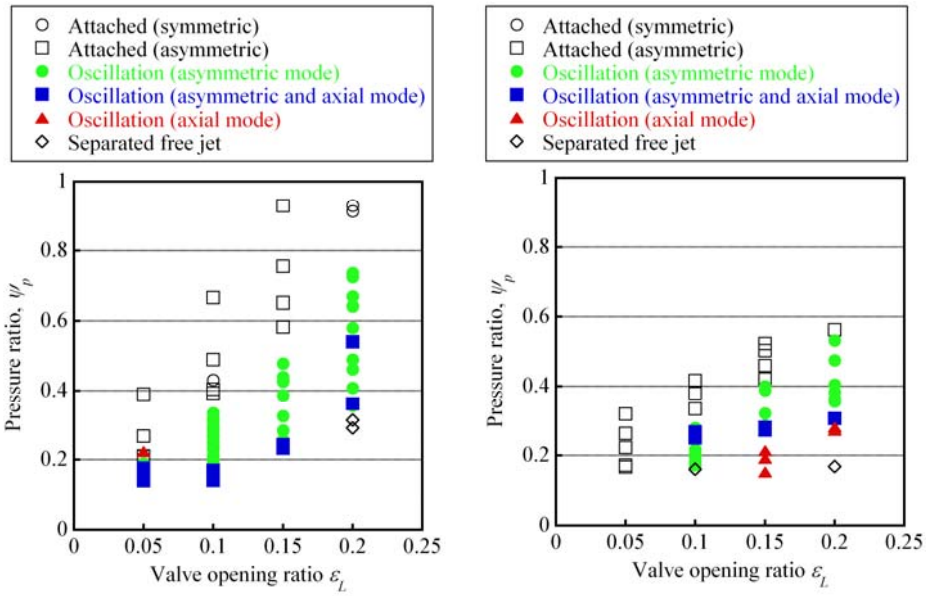


(a) Larger model (b) Smaller model

**Fig. 9** Flow patterns indicated on $\varepsilon_L - \psi_p$ plane (Experiment)

Separated free jet

Fig. 8 shows the flow field and the pressure fluctuations for the case with separated free jet. At the smaller pressure ratio, the separated jet become static and the wall pressure fluctuation becomes small.

Observed flow patterns indicated in $\varepsilon_L - \psi_p$ plane for the larger model and smaller model in Fig. 9. The attached flow pattern is observed smaller $\varepsilon_L$ and larger $\psi_p$. The separated free jet pattern is observed at larger $\varepsilon_L$ and smaller $\psi_p$. The flow oscillation appears between the regions with separated and attached flow patterns. The boundaries of the regions of each pattern are different at smaller and larger models. This will be discussed later.

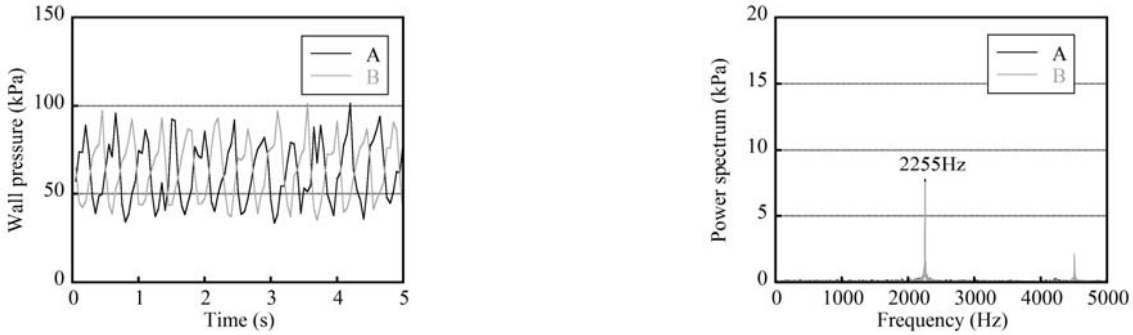


(a) Wall Pressure measurement of valve head (b) FFT result of pressure fluctuation of valve head

**Fig. 10** Wall pressure measurement (Smaller model, $\varepsilon_L$=0.20, $\psi_p$=0.36)

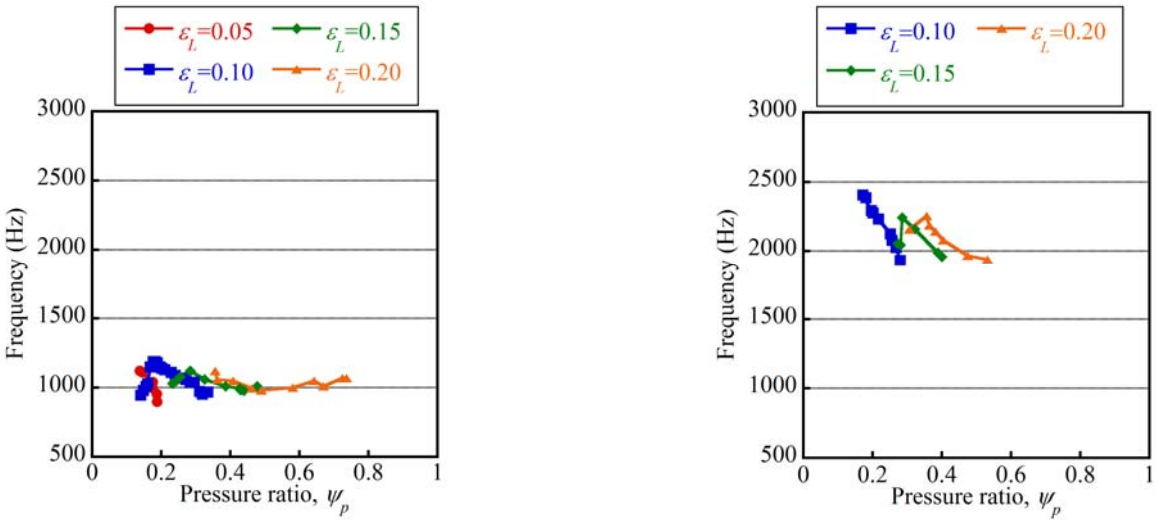


(a) Larger model (b) Smaller model

**Fig. 11** Frequency of asymmetric mode of pressure fluctuation versus pressure ratio for various valve opening ratios

### 4.2 Scale Effect on Asymmetric Flow Oscillation

Fig. 10 shows the pressure fluctuations at $\varepsilon_L$=0.20 and $\psi_p$=0.36 with the smaller model. The amplitude of the pressure fluctuation is similar to the case of the larger model shown in Fig. 6. The reason why the amplitude of the pressure fluctuation is not affected by the scale is explained by normalizing the pressure.

$$\Delta p^* = \frac{\Delta p}{\left(\frac{1}{2}\rho U^2\right)} \tag{4}$$

Here, $\Delta p$ is the amplitude of the pressure fluctuation, $\rho$ is a representative density, and $U$ is a representative velocity. In the present experiment, $\rho$ and $U$ are depend on the pressure ratio, $\psi_p$. Therefore, the model size does not affect the normalized pressure.

The frequency of the asymmetric mode of the pressure fluctuation is plotted against pressure ratio in Fig. 11. The frequency in the larger model is about the half of that in smaller model. This reason is explained by considering the following definition of Strouhal number.

$$St = \frac{fL}{U} \tag{5}$$

Here, $f$ is frequency of the pressure fluctuation, $L$ is a representative length and $U$ is a representative velocity. In the present experiment, $U$ does not depend on the scale of the experimental model because the inlet pressure and temperature are the same for both models. The frequency $f$ of the larger model is almost a half of the smaller model as shown in Fig. 11. The height of downstream duct, $h_D$ of the larger model is two time larger than that of the smaller model as shown in Table 1. Therefore, the frequency is inversely proportional to the height of the downstream duct.

In Fig. 11, another scale effect is observed. The range of the pressure ratio where the pressure fluctuation appears is wider in the larger model than in the smaller model. This difference is caused by the difference of Reynolds number as examined in the next section with numerical results.

## 5. Numerical Results

### 5.1 Flow Oscillation

In order to discuss about the flow field, two-dimensional unsteady numerical simulations are carried out for the case of asymmetrically oscillating flow.

Fig. 12 shows the pressure fluctuation and its spectra at $\varepsilon_L$=0.20 and $\psi_p$=0.35. By comparing with the experimental result shown in Fig. 6, the numerical result is in acceptable agreement in both amplitude and frequency. The phase difference between points A and B is almost 180 degrees as observed in the experimental result. Similar agreements are shown at other conditions. From numerical results, the averaged speed of sound downstream the valve head is evaluated to be about 300 m/s. From the frequency of 1074 Hz and the speed of sound of 300 m/s, the wave length of the acoustic pressure wave is calculated to be 0.28m. This is almost double of the duct height. Therefore, it is considered that the flow oscillation is affected by the acoustic resonance in height direction of the duct.

Fig. 13 shows the Mach number distribution and the velocity vector at each 1/4 period of the flow oscillation. Two jets

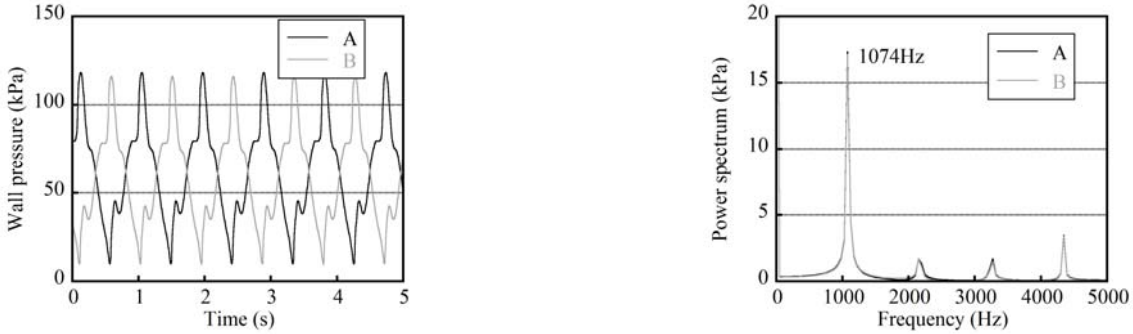


(a) Wall Pressure measurement of valve head (b) FFT result of pressure fluctuation of valve head

**Fig. 12** Numerical result of wall pressure fluctuation (larger model, $\varepsilon_L$=0.20 and $\psi_p$=0.35)

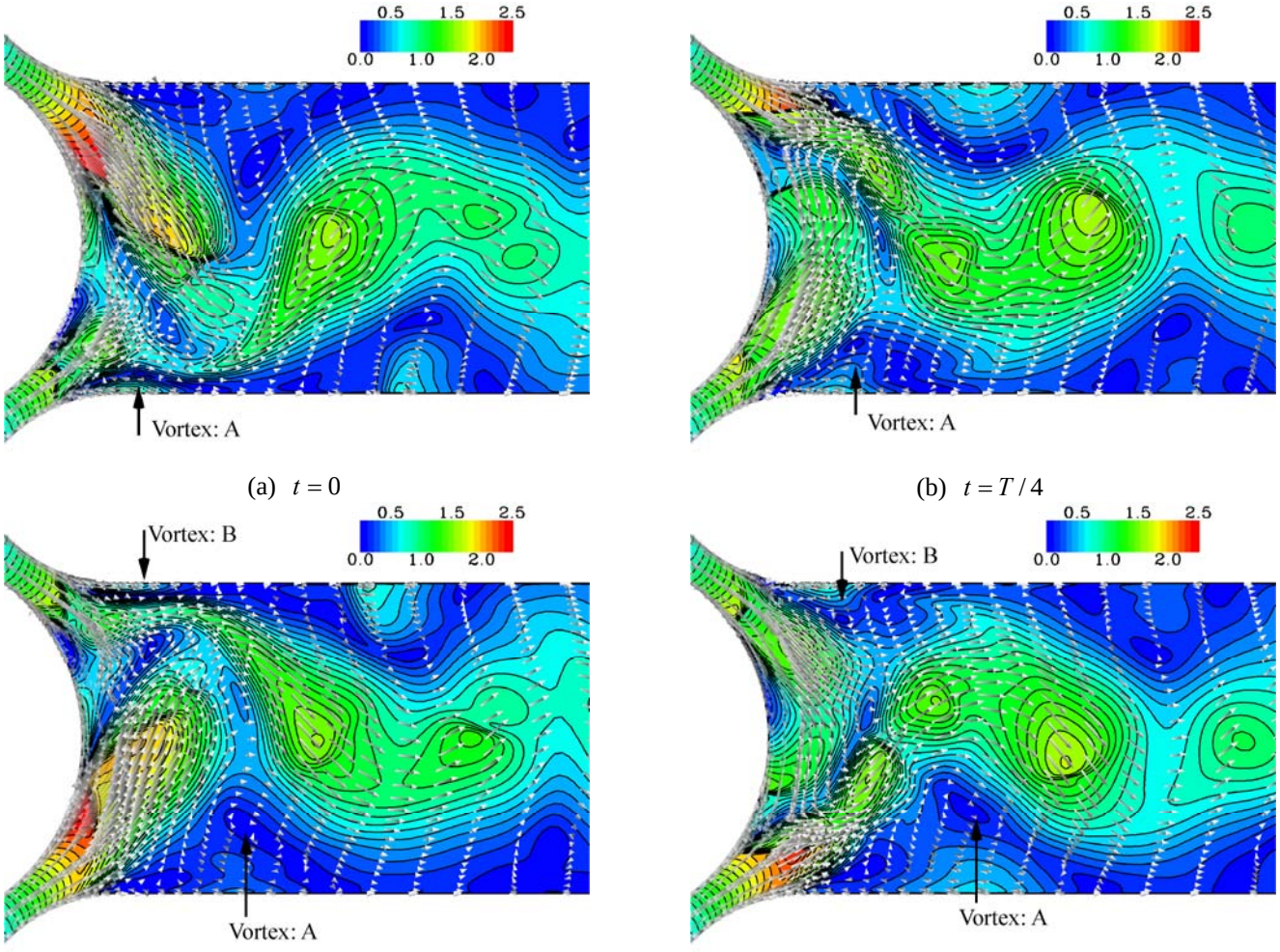


(a) $t = 0$ (b) $t = T/4$

(c) $t = 2T/4$ (d) $t = 3T/4$

**Fig. 13** Mach number distribution and velocity vector field at each 1/4 period of flow fluctuation (Larger model, $\varepsilon_L$=0.20 and $\psi_p$=0.35)

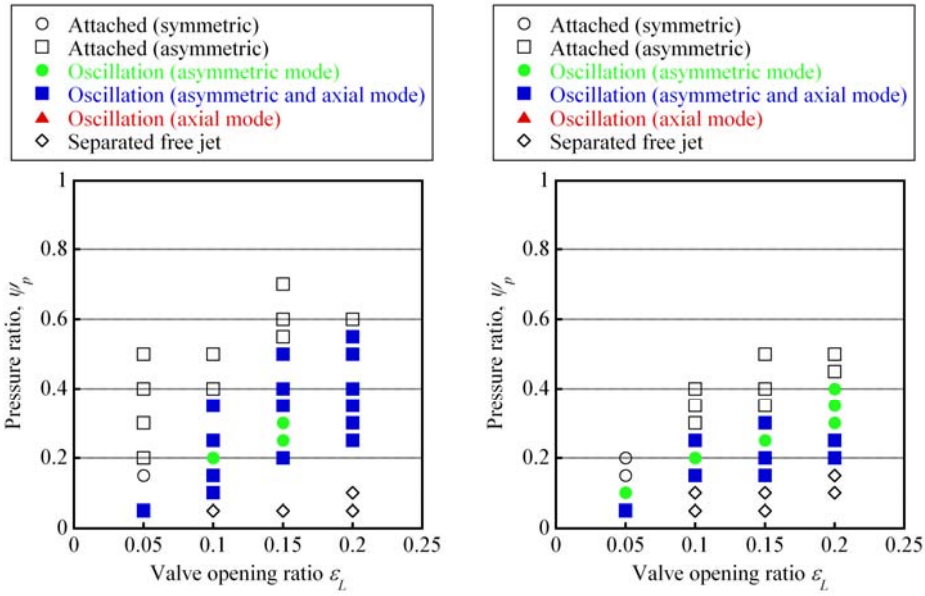


(a) Larger model (b) Smaller model

**Fig. 14** Flow patterns indicated on $\varepsilon_L - \psi_p$ plane (Numerical result)

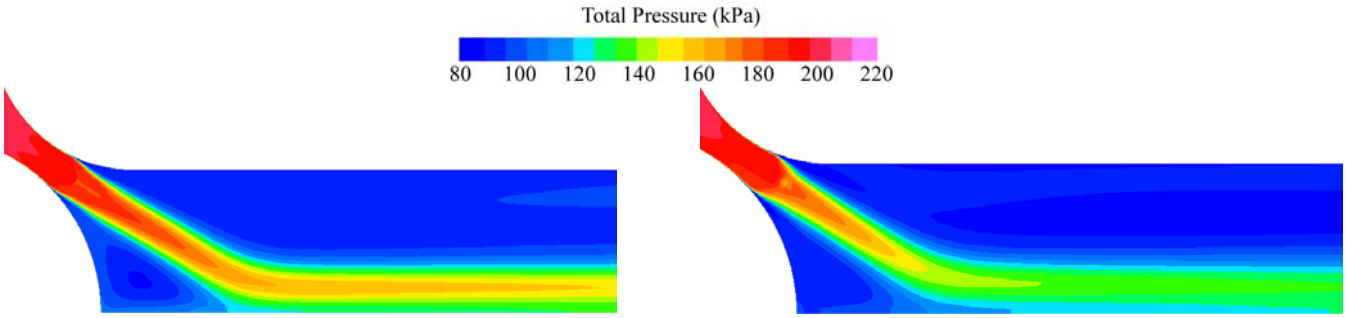


(a) Larger model (b) Smaller model

**Fig. 15** Total pressure distribution (Numerical results, $\varepsilon_L$=0.20 and $\psi_p$=0.50)

oscillate with shocks alternatively. A vortex indicated as “Vortex: A” in Fig. 13 (a) appears from the separation point on the lower valve seat. The lower jet becomes larger as the “Vortex: A” becomes larger as shown in Fig. 13 (b). In Fig. 13 (c), the “Vortex: A” moves downstream and a new vortex “Vortex: B” appears at the separation points on the upper valve seat. In Fig. 13 (d), “Vortex: A” moves further downstream without significant deformation. Strouhal numbers of the flow fluctuations in the duct defined with duct height and axial velocity are not constant because the frequencies are almost constant in all conditions but the velocities are varied depending on the pressure ratio and the valve opening ratio. From these observations, the flow fluctuation near the valve head is caused by the acoustic resonance of the jet. In more downstream of the valve head, on the other hand, the flow fluctuates because of the movement of vortices caused by the flow fluctuation near the valve head.

### 5.2 Influence of Reynolds number

In Fig. 14, the flow patterns are indicated in $\varepsilon_L - \psi_p$ plane for the larger model and smaller model. By numerical simulations, the flow oscillation with only axial mode was not observed. However, the regions of each pattern by numerical results agree with experimental results. As was in experiments shown in Fig. 9, numerical results show that the flow oscillation appears in wider region in the larger model than in the smaller model.

Numerical simulations with half computational domains in height direction are carried out in order to understand the cause of the scale effect on the appearance of the flow oscillation. Fig. 15 shows the comparison of the total pressure distribution between the larger and smaller models. In the smaller model, the total pressure of the jet decreases more largely than in the larger model. This is caused by the difference of Reynolds number. Comparing with the larger model, in the smaller model, the jet becomes more stable and attaches at lower pressure ratios because the momentum of the jet is smaller than in the larger model. In the smaller model, therefore, the region of $\varepsilon_L - \psi_p$ plane where the reattached flow pattern appears becomes larger.

## 6. Concluding remarks

Flow characteristics in the steam control valve are investigated by experiments and numerical simulations with two-dimensional valve models. The flow patterns are classified into the attached steady flow, the oscillating flow and the separated free jets. The reattached flow and the separated free jet are almost steady. The reattached flow appears at relatively high pressure

ratio and the separated free jet appears at low pressure ratio. The flow oscillation appears between them.

Scale effects of the valve on the flow oscillation are also examined by comparing the result with two similar models with different size. The amplitude of the pressure fluctuation is not affected by the scale. The frequency of the flow oscillation is inversely proportional to the height of downstream duct. The model size affects the range of the valve operating condition with the flow oscillation.

Numerical results show quantitative agreement with experimental results. From the flow field by numerical simulations, the flow fluctuation near the valve head is found to be caused by the acoustic resonance of the jet. On the other hand, in more downstream, the flow fluctuation occurs because of the movement of vortices caused by the flow fluctuation near the valve head. The numerical result also shows that the influence of Reynolds number is caused by the difference of the total pressure of the jet.

## 7. Nomenclature

| | | | |
|---|---|---|---|
| $D_s$ | Seat diameter | $R_H$ | Curvature radius of valve seat |
| $h_D$ | Height of downstream duct | $w_D$ | Depth of downstream duct |
| $L_D$ | Length of downstream duct | $x_L$ | Lift of valve head |
| $p_{01}$ | Inlet pressure | $\varepsilon_L$ | Valve opening ratio |
| $p_2$ | Back pressure | $\psi_p$ | Pressure ratio |
| $R_H$ | Curvature radius of valve head | | |

## 8. References


[1] Widel, K.-E., 1980, “Governing Valve Vibrations in a Large Steam Turbine,” Practical Experiences with Flow-Induced Vibrations, Springer-Verlag, New York, pp. 320-322.

[2] Araki, T., Okamoto, Y. and Otomo, F., 1981, “Fluid-Induced Vibration of Steam Control Valves (In Japanese),” Toshiba Review, Vol. 36, No. 7, pp. 648-656.

[3] Jibiki, K., 2000, “Fluctuation of Steam Control Valve (In Japanese),” Turbomachinery, Vol. 28, No. 4, pp. 225-229.

[4] Morita R., Inada F., Mori M., Tezuka K., and Tsujimoto Y., 2007, “CFD Simulations and Experiments of Flow Fluctuations Around a Steam Control Valve,” Journal of Fluids Engineering 129, 48, pp. 48-57.

[5] Yee, H., 1987, “Upwind and Symmetric Shock-Capturing Schemes,” NASA-TM-89464.

[6] Takakura, Y., Ogawa, S., *et al.*, 1989, “Turbulence Models for 3D Transonic Viscous Flows,” Proc. AIAA 9th Comp. Fluid Dynamics Conf., 89-1952-CP, pp. 240–248.

[7] Yoon, S., and Jameson, A., 1988, “Lower-Upper Symmetric-Gauss-Seidel Method for the Euler and Navier-Stokes Equations,” AIAA Journal, 26(9), pp. 1025-1026.